Title
Adaptive Downregulation of Mitochondrial Function in Down Syndrome

Journal
Cell Metabolism, 17(1)

ISSN
1550-4131

Authors
Helguera, Pablo
Seiglie, Jaqueline
Rodriguez, Jose
et al.

Publication Date
2013

DOI
10.1016/j.cmet.2012.12.005

Published in final edited form as:
Cell Metab. 2013 January 8; 17(1): 132–140. doi:10.1016/j.cmet.2012.12.005.

Adaptive Downregulation of Mitochondrial Function in Down Syndrome

Pablo Helguera[1,6], **Jaqueline Seiglie**[1], **Jose Rodriguez**[4], **Michael Hanna**[1], **Gustavo Helguera**[5], and **Jorge Busciglio**[1,2,3]

[1]Department of Neurobiology and Behavior, University of California, Irvine, CA 92697

[2]Institute for Memory Impairments and Neurological Disorders (iMIND), University of California, Irvine, CA 92697

[3]Center for the Neurobiology of Learning and Memory (CNLM), University of California, Irvine, CA 92697

[4]Molecular Biology Institute, University of California, Los Angeles, CA 90095

[5]Cátedra de Tecnología Farmacéutica I, Facultad de Farmacia y Bioquímica, Universidad de Buenos Aires, Junín 954 6° Piso, C1113AAD, Ciudad Autónoma de Buenos Aires, Argentina

[6]Laboratorio de Neuropatologia Experimental, Instituto de Investigación Médica Mercedes y Martín Ferreyra, INIMEC-CONICET, Universidad Nacional de Córdoba, Friuli 2434, 5016 Córdoba, Argentina

SUMMARY

Mitochondrial dysfunction and oxidative stress are common features of Down syndrome (DS). However, the underlying mechanisms are not known. We investigated the relationship between abnormal energy metabolism and oxidative stress with transcriptional and functional changes in DS cells. Impaired mitochondrial activity correlated with altered mitochondrial morphology. Increasing fusion capacity prevented morphological but not functional alterations in DS mitochondria. Sustained stimulation restored mitochondrial functional parameters but increased ROS production and cell damage, suggesting that reduced DS mitochondrial activity is an adaptive response to avoid injury and preserve basic cellular functions. Network analysis of genes overexpressed in DS cells demonstrated functional integration in pathways involved in energy metabolism and oxidative stress. Thus, while preventing extensive oxidative damage, mitochondrial downregulation may contribute to increased susceptibility of DS individuals to clinical conditions in which altered energy metabolism may play a role such as Alzheimer's disease, diabetes, and some types of autistic spectrum disorders.

Keywords

Down syndrome; mitochondria; oxidative stress; mitochondrial fission and fusion; human aneuploidy; axonal transport; pancreatic β cells

Correspondence: Jorge Busciglio, Department of Neurobiology and Behavior, University of California-Irvine, 3216 BioSci III, Irvine, CA 92697-4545. Tel. (949) 824-4820. jbuscigl@uci.edu.

INTRODUCTION

Down Syndrome (DS) or trisomy 21, is characterized by a complex phenotype that includes both developmental and chronic health complications (Roizen and Patterson, 2003). Altered mitochondrial activity and oxidative stress have long been associated with DS (Arbuzova et al., 2002; Brooksbank and Balazs, 1984)

For example, DS cortical neurons exhibit higher production of intracellular reactive oxygen species (ROS) and lipid peroxidation, which compromise neuronal survival (Busciglio and Yankner, 1995), and both DS neurons and astrocytes display an abnormal pattern of protein processing consistent with chronic energy deficits (Busciglio et al., 2002). Altered mitochondrial activity has been reported in DS fibroblasts (Valenti et al., 2011) and mitochondrial DNA mutations were found in DS brain tissue (Coskun and Busciglio, 2012).

Microarray profiling of DS neural progenitor cells indicates an association between altered chromosome 21-gene expression and cellular injury mediated by oxidative stress (Esposito et al., 2008). Similarly, DS amniotic fluid samples show altered activity of oxidative stress-associated genes early in pregnancy (Slonim et al., 2009).

Oxidative stress has been widely associated with impaired mitochondrial function and morphology, leading to disruption of cable-like morphology and impaired ATP production (Knott et al., 2008). Functional elongated mitochondria undergo remodeling in response to energy requirements, cellular stress or calcium oscillations (Chan, 2006), and mitochondrial fragmentation is correlated with reduced ATP and increased ROS production (Yu et al., 2006). With these considerations in mind, we assessed the relation between mitochondrial dysfunction, altered mitochondrial morphology, oxidative stress and transcriptional changes in DS cells. The results indicate that reduced mitochondrial metabolism in DS is associated with an adaptive response to prevent oxidative damage and preserve cellular function.

RESULTS

Altered morphology and increased oxidative stress in DS mitochondria

There is a close relationship between mitochondrial morphology and functional state. Marked alterations in mitochondrial function previously identified in DS cells (Busciglio et al., 2002) led us to examine mitochondrial morphology in NL and DS astrocytes (Fig 1A). Mitochondria were classified according to size in three groups: ≤3 μm, 3.1–15 μm and ≥15.1 μm. The mitochondrial network in DS cells is more fragmented, as demonstrated by a significant increase in the number of shorter mitochondria (both ≤3 μm and 3.1–15 μm groups) and reduced number of longer mitochondria (≥15.1 μm)(Fig 1B). Electron transport chain protein expression was similar in NL and DS cells (SFig 1A), indicating that morphological and functional changes were not related to changes in DS mitochondrial mass. We found shorter mitochondria in other DS primary cell types, including fibroblasts (SFig 1B), neurons (Fig 3) and pancreatic cells (Fig 4), suggesting generalized perturbations in DS mitochondrial function and morphology. Altered mitochondrial morphology is associated with functional impairment in DS cells, which exhibit reduced MMP, oxidoreductase (ox/red) activity and ATP generation (Busciglio et al., 2002). Given the close association between mitochondrial morphology and function, we investigated whether functional changes could be reverted by manipulating DS mitochondrial morphology. Mitofusin 1 (mfn1), a critical regulator of mitochondrial fusion, enhanced DS mitochondrial fusion (Fig 1C), increased the number of tubular mitochondria, and reduced the number of puncta-like ones (Fig 1D). However, mfn1 expression had no effect on MMP (Fig 1E and F). Similar results were obtained with mfn2 (data not shown)

Since correcting morphological alterations did not enhance DS mitochondrial function, we investigated whether DS cells actually possess the capacity to increase mitochondrial activity after metabolic stimulation. To achieve a sustained stimulation of mitochondria, we used 5 mM creatine for seven days (Andres et al., 2005). ATP level, ox/red activity and MMP were reduced in DS cells (Fig 1G, H and I). Creatine did not affect mitochondrial activity in NL cells but it markedly increased ox/red activity, ATP levels and MMP in DS cells (Fig 1G, H and I), indicating that upon stimulation, DS mitochondria possess the capacity to increase energy metabolism. However, creatine reduced DS cell survival while it had no effect in the viability of NL cultures (Fig 1J). One potential consequence of enhanced mitochondrial activity is increased free radical generation, which has been previously reported in DS (Busciglio & Yankner, 1995). Under basal conditions, DS cells exhibited 3-fold higher levels of superoxide expressed as the ratio of MitoSox red over Mitotracker green fluorescence area (NL: 4±1%, DS: 16±3%)(Fig 1K and L). Creatine nearly doubled superoxide levels in both NL and DS mitochondria (NL: 12±5% NL, DS: 31±9%)(Fig 1L). In addition, creatine increased lipid peroxidation in DS cells (Fig 1M), consistent with the observed decrease in cell viability (Fig 1J). Thus, DS mitochondria are capable of sustaining increased activity. However, it resulted in increased ROS generation, cellular damage and cell death.

Gene expression in DS cells is associated with a pattern of chronic oxidative stress

We performed a broad-spectrum microarray analysis using mRNA from 3 NL and 5 DS astrocyte cultures. The microarray output was validated for several genes (SFig 2A and SMethods). 92 genes discriminated between NL and DS samples (Fig 2A). 60 genes were upregulated (>1.45 fold), 11 of which are located in chromosome 21 (highlighted in red, Fig 2A). The other 32 genes were downregulated (<0.65 fold), none of which is localized in chromosome 21. Although chromosome 21 genes were overrepresented among upregulated genes (18.3%), the majority of them (81.7%) were located in other chromosomes.

Ingenuity analysis generated a network illustrating the relationship between overexpressed genes (SFig 2B). Three main pathways related to the upregulated genes were identified: 1-Nfr2-associated oxidative stress response, 2- oxidative stress, and 3- mitochondrial dysfunction (SFig 2B). All 3 pathways support the presence of chronic oxidative stress in DS. To explore the relation between gene expression and oxidative stress, we evaluated the expression of “DS signature genes” in NL astrocytes subjected to mild oxidative stress (50 μM H_2O_2 for 12 hr). In general, the changes in “DS signature genes” in NL astrocytes +H_2O_2 were smaller in magnitude than the ones in DS cells. However, in most cases, the expression in NL astrocytes+H_2O_2 shifted in the same direction as in DS cells, placing their profile somewhere between the DS and NL profiles (Fig 2B) and further suggesting that oxidative stress drives gene expression changes in DS cells.

Altered mitochondrial morphology and function in DS neurons

Since cells with high energy demands are especially susceptible to mitochondrial alterations, we assessed mitochondrial function in DS neurons.

Mitochondria were classified according to size as: puncta-like mitochondria (≤300 nm in diameter)(Fig 3A, small arrow); globular mitochondria, (600 to 1200 nm in diameter)(Fig 3A, arrow head); and tubular mitochondria (≥500 nm)(Fig 3A, big arrow). Mitochondria were also shorter in DS neurons (Fig 3B). Similar results were obtained using Mitotracker green and JC-1 (SFig 3A and B). JC-1 labeling revealed a marked reduction in MMP, which was accompanied by decreased ox/red activity and ATP levels (Fig 3C and SFig 3D and E). JC-1 formed aggregates in discrete domains of tubular and puncta-like mitochondria but never in globular mitochondria (SFig 3B), which frequently colocalized with lisosomal

markers (SFig 3C), suggesting that the latter represent a subset of inactive or damaged mitochondria. Interestingly, discrete energized regions in both NL and DS mitochondria (SFig 3B and D) point to the existence of specific domains with different activity within individual mitochondria in human neurons.

Impaired mitochondrial transport in DS neurons

Since axonal transport is highly dependent on ATP and it is critical for synaptic activity and neuronal survival (Brady, 1991), we assessed anterograde mitochondrial transport in DS neurons. DS mitochondria moved slower (350±60 nm/sec) than NL mitochondria (1,100±130 nm/sec, Fig 3D and E). Conversely, we observed a higher number of moving mitochondria at any given time point in DS cells (38±7% in DS cells; 20±3% in NL cells; Fig 3F), which may be a compensatory change. Both parameters were affected by creatine, which also increased the number of energized mitochondria in DS neurons (SFig 3E). Thus, reduced mitochondrial function and ATP levels lead to impaired mitochondrial transport in DS neurons.

Functional alterations in DS pancreatic β cells are associated with reduced energy metabolism

Pancreatic cells also require relatively high metabolic rates to maintain secretory function. We examined mitochondrial morphology, activity and basal insulin secretion in NL and DS islet cell clusters (ICC)(Fig 4A). Both fetal pancreas and ICC expressed insulin and glucagon (Fig 4B, I and II). Mitochondria in β cells were visualized with anti-cytochrome C (Fig 4C). DS β cells exhibited fragmented mitochondria (DS, Fig 4D), as did NL β cells treated with 5 μM CCCP for 1 hr (NL+FCCP, Fig 4D). Oxido/reductase activity was reduced in DS ICC (73%±9% of NL ICC activity normalized as 100%). Since mitochondrial dysfunction is associated with intracellular amyloid β accumulation in DS cells (Busciglio et al., 2002), we assessed whether islet amyloid polypeptide (IAPP or amylin) accumulates in DS β cells. Insulin and IAPP are coexpressed and localize to the same vesicles in β cells (Fig 4E), which were labeled with A11, a conformation-specific antibody that recognizes IAPP oligomers (Kayed et al., 2007). We found increased A11-positive puncta in DS β cells, 7.3±2.6 puncta/cell in DS cells and 1.7±1.5 puncta/cell in NL cells, n=5 in both cases (Fig 4F, arrows). Thus, energy deficits may result in abnormal intracellular accumulation of IAPP in DS β cells. NL β cells secreted 4-fold more insulin than DS β cells (Fig 4G). In contrast, DS β cells secreted 8-fold more proinsulin than NL β cells (Fig 4H), indicating incomplete processing and reduced insulin secretion. Neither creatine (5mM) nor trolox (50 μM) alone had an effect on insulin or proinsulin secretion. However when both compounds were added together, we observed a slight increase in insulin (17 ± 5%) and a reduction in proinsulin (24 ± 4%) secretion in DS ICC (Fig 4G and H). None of the treatments had significant effect in insulin or proinsulin levels in NL cells (data not shown). Thus, mitochondrial downregulation may impair secretory function in DS β cells. The secretory deficits were partially corrected by combined treatment with an energy buffer and an antioxidant, underscoring the link between impaired cellular function, oxidative stress and mitochondrial alterations in DS.

DISCUSSION

Chronic oxidative stress and mitochondrial dysfunction are conspicuous features of DS (Arbuzova et al., 2002; Slonim et al., 2009). We found that mitochondrial morphology is consistently altered in DS cells, which exhibit increased fragmentation. Mitofusin overexpression reverted the fragmented phenotype. However, it did not improve MMP in DS cells. Consequently, we investigated whether DS mitochondria actually possessed the capacity to increase ATP production after metabolic stimulation. Creatine increased DS

mitochondrial activity and mitochondrial anterograde movement, but it nearly doubled ROS levels, increased lipid peroxidation and reduced viability in DS cells. Thus, sustained stimulation resulted in increased DS cell damage and death, suggesting that the downregulation of DS mitochondria is part of an adaptive response to avoid excessive ROS generation and cellular injury.

From a broader perspective, the relation between mitochondrial morphology and function appears to be context-specific, depending on the cell's state and the factors affecting it. For example, in insulinoma cells, ATP-dependent hormone secretion is not affected by induced mitochondrial fragmentation with a dominant negative form of mfn1 but is significantly reduced by hFis1 overexpression, which also generates a fragmented phenotype (Park et al., 2008). In the case of DS primary cells, mitochondria are more fragmented and both energy production and some cellular functions are impaired. Thus, the balance between mitochondrial morphology and function is complex and it is influenced by multiple factors.

We found 92 genes differentially expressed in DS cells. Ingenuity analysis generated a network of overexpressed genes indicative of a transcriptional response to oxidative stress (SFig 2). These changes in gene expression may orchestrate the cellular adaptations required to preserve homeostasis in DS cells, including downregulation of energy metabolism. This possibility is further supported by similar although less pronounced changes in the expression of "DS signature genes" in NL astrocytes under mild oxidative stress (Fig 4B). Under basal culture conditions, which are nevertheless pro-oxidant, and where DS energy metabolism is already impaired (Coskun and Busciglio, 2012; Valenti et al., 2011), the adaptive response would stabilize cell homeostasis at the expense of compromising cellular functions dependent on particular energy requirements, e.g. insulin secretion in β cells or axonal transport in neurons. At the organismal level, this adaptation may contribute to the increased susceptibility of DS individuals to pathologies in which energy metabolism appears to be compromised such as Alzheimer's disease, diabetes, and some forms of autism (Capone et al., 2005; Esbensen, 2010; Lott and Head, 2005).

Recent studies have underscored the critical role of chronic superoxide production leading to mitochondrial dysfunction, telomere shortening and replicative senescence in human cells (Passos et al., 2007), further suggesting that the accelerated senescence phenotype characteristic of DS cells (Pallardo et al., 2010) may also be a direct result of cumulative oxidative damage and mitochondrial mutations (Coskun and Busciglio, 2012). Aneuploidies in general are detrimental to organismal and cellular function, altering cell metabolism and decreasing cell proliferation in yeast, mice and humans, regardless of which chromosome is affected (Williams et al., 2008). In fact, human fibroblasts harboring different aneuploidies display similar increased sensitivity and common cellular responses to chronic oxidative stress (Helguera and Busciglio, unpublished result). In this context, DS phenotypes at both cellular and system levels would arise from the interplay between specific changes in chromosome 21-gene expression operating on a background of generalized metabolic perturbations set off by the aneuploid state.

In summary, DS cells exhibit chronic energy deficits that appear to be part of an adaptive response to minimize oxidative damage and preserve cellular homeostasis. Depending on particular energy requirements, specific cellular functions will be affected in different cell types. In the case of DS pancreatic β cells, insulin secretion and proinsulin processing were significantly improved only when antioxidant treatment and mitochondrial stimulation were applied together. Thus, combined therapeutic strategies directed to prevent free radical damage while modulating energy metabolism may prove valuable for managing some of the clinical manifestations commonly associated with DS.

METHODS

Cell cultures

primary human cortical neuronal and astrocyte cultures were established from 10 DS (17–20 weeks of gestational age) and 10 age-matched control brain samples (Busciglio et al., 2002). The protocol for tissue procurement complied with Federal and Institutional guidelines for fetal research. Each experiment was replicated with at least 5 different normal and DS cultures. For most experiments, cortical neuronal and astrocyte cultures were used at 30–35 days in vitro. Fetal pancreatic cultures were generated from NL and DS fetal pancreases as described (Beattie et al., 1997). Mitochondrial and endocrine precursor cell function were analyzed at day 5 in culture.

Imaging

fluorescent images were generated with a Zeiss Axiovert 200 inverted microscope, and image analysis was performed with Axiovision software costumized macros. Mitochondria were classified in length intervals or according to pre-determined sizes as punctate, tubular and globular, and scored using Axiovision. Mitochondrial transport and quantification of mobile mitochondria were measured by time-lapse image analysis after a 20 min incubation with 100 nM Mitotracker green (detailed in Supplemental Methods).

Assessment of mitochondrial function

mitochondrial ox/red was measured using the MTS assay (Promega, Madison, WI, USA). JC-1 (Invitrogen) was used to assess mitochondrial membrane potential (MMP) as a ratio between JC1 red area (high MMP mitochondria) and JC1 green area (total mitochondria) after incubation with 200 nM JC1 for 20 min. An LDH assay was used to assess cell density (CytoTox 96®, Promega). ATP levels were measured using chemiluminescence (Cell titer Glo, Promega). For all experiments, lipid peroxidation, ox/red and ATP levels were normalized to LDH cellular levels or total protein content. Both normalization methods gave similar results.

Transfection

cells were transfected with Lipofectamine (Invitrogen) and the plasmid of interest in a ratio of 0.4 μg of DNA plus 1 μl of Lipofectamine per 500 μl of medium. Full-length mitofusin 1 (pmfn1) and mitofusin 2 (pmfn2) plasmids (Origene, Rockville, MD, USA) and mitochondrial targeted cyan fluorescent protein (pCFPmit) vector, (Clontech, Palo Alto, CA, USA) were confirmed by sequencing. Plasmid concentrations were selected after performing dose-response curves to find optimal conditions to stimulate fusion but avoiding hyperfusion of the mitochondrial network. None of the vectors caused hyperfusion nor they affected cell viability at the indicated concentrations.

Immunocytochemistry

cell cultures and ICCs were fixed with 4% paraformaldehyde/0.12 M sucrose in PBS and permeabilized with 0.1% Triton X-100 in PBS. Immunofluorescent preparations were visualized using Alexa-conjugated secondary antibodies (Invitrogen), as previously described (Helguera et al., 2005; Beattie et al., 1997). The following primary antibodies were used: sheep anti-cytochrome C (Abcam, Cambridge, UK), rabbit anti-insulin (clone C27C9, Cell Signaling, Danvers, MA, USA), mouse anti-IAP (Serotec, Raleigh, NC, USA), conformation-specific anti-oligomeric amyloid (A11, kindly provided by Dr C. Glabe, UCI).

Gene expression

profiles were generated using total mRNA from normal astrocytes (NL), normal astrocytes treated with H2O2 (50 μM for 24 hr) and DS astrocytes, and hybridized onto HumanRef-8 v2 Expression BeadChips (Illumina). See Supplemental Methods for technical details.

ELISA

commercial kits for insulin (ALPCO Diagnostics, Windham, NH, USA) and pro-insulin (LIMCO Research, St. Charles, MO, USA) were used according to manufacturer's instructions. Conditioned media from NL and DS floating ICC were sampled after 5 days in culture.

Oxidative stress

mitochondrial superoxide was visualized using MitoSox red (Invitrogen), which emits red fluorescence when oxidized by superoxide. Cells were treated with MitoSox red (200 nM) for 10 min and co labeled with Mitotracker green (100 nM). The red/green ratio was used as an indicator of superoxide production per mitochondrial mass. Lipid peroxidation was detected using diphenyl-1-pyrenylphosphine (DPPP, Molecular Probes- Invitrogen). DPPP fluorescence was quantified in a Spectramax fluorometer (Molecular Devices).

Creatine treatment

cortical cultures were treated with 5 mM creatine for 7 days. ICCs were treated with 5 mM creatine for 2 days. (See Supplemental Methods).

Statistical procedures

Data were analyzed by one-way analysis of variance (ANOVA) followed by Tukey's HSD test, when the experiment included three or more groups; and two-way ANOVA followed by Tukey's HSD test for assays with two independent variables. Student's ***t*** test was performed for paired observations. A value of $p<0.05$ was considered statistically significant. Results were expressed as the mean ± standard deviation (SD). All experiments were repeated at least 3–5 times using cultures derived from different NL and DS specimens. Each individual experiment was performed at least in triplicate samples.

Supplementary Material

Refer to Web version on PubMed Central for supplementary material.

Acknowledgments

We thank Drs Alberto Hayek (UCSD), Peter Butler (UCLA) and Alfredo Lorenzo (IMMF, CONICET, UNC) for expert advice. Drs Pablo Helguera and Gustavo Helguera are members of the National Council for Scientific and Technological Research (CONICET), Argentina. Supported by grants from The Larry L. Hillblom Foundation and NIH (HD38466) and Alzheimer's Disease Research Center grant (AG16573).

References

Andres RH, Ducray AD, Huber AW, Perez-Bouza A, Krebs SH, Schlattner U, Seiler RW, Wallimann T, Widmer HR. Effects of creatine treatment on survival and differentiation of GABA-ergic neurons in cultured striatal tissue. J Neurochem. 2005; 95:33–45. [PubMed: 16045451]

Arbuzova S, Hutchin T, Cuckle H. Mitochondrial dysfunction and Down syndrome. Bioessays. 2002; 24:681–684. [PubMed: 12210526]

Beattie GM, Cirulli V, Lopez AD, Hayek A. Ex vivo expansion of human pancreatic endocrine cells. J Clin Endocrinol Metab. 1997; 82:1852–1856. [PubMed: 9177395]

Brady ST. Molecular motors in the nervous system. Neuron. 1991; 7:521–533. [PubMed: 1834098]

Brooksbank BW, Balazs R. Superoxide dismutase, glutathione peroxidase and lipoperoxidation in Down syndrome fetal brain. Brain Res. 1984; 318:37–44. [PubMed: 6237715]

Busciglio J, Pelsman A, Wong C, Pigino G, Yuan M, Mori H, Yankner BA. Altered metabolism of the amyloid beta precursor protein is associated with mitochondrial dysfunction in Down syndrome. Neuron. 2002; 33:677–688. [PubMed: 11879646]

Busciglio J, Yankner BA. Apoptosis and increased generation of reactive oxygen species in Down syndrome neurons in vitro. Nature. 1995; 378:776–779. [PubMed: 8524410]

Capone GT, Grados MA, Kaufmann WE, Bernad-Ripoll S, Jewell A. Down syndrome and comorbid autism-spectrum disorder: characterization using the aberrant behavior checklist. Am J Med Genet A. 2005; 134:373–380. [PubMed: 15759262]

Chan DC. Mitochondria: dynamic organelles in disease, aging, and development. Cell. 2006; 125:1241–1252. [PubMed: 16814712]

Coskun PE, Busciglio J. Oxidative Stress and Mitochondrial Dysfunction in Down's Syndrome: Relevance to Aging and Dementia. Current gerontology and geriatrics research. 2012; 2012:383170. [PubMed: 22611387]

Esbensen AJ. Health conditions associated with aging and end of life of adults with Down syndrome. Int Rev Res Ment Retard. 2010; 39:107–126. [PubMed: 21197120]

Esposito G, Imitola J, Lu J, De Filippis D, Scuderi C, Ganesh VS, Folkerth R, Hecht J, Shin S, Iuvone T, Chesnut J, Steardo L, Sheen V. Genomic and functional profiling of human Down syndrome neural progenitors implicates S100B and aquaporin 4 in cell injury. Hum Mol Genet. 2008; 17:440–457. [PubMed: 17984171]

Helguera P, Pelsman A, Pigino G, Wolvetang E, Head E, Busciglio J. ets-2 promotes the activation of a mitochondrial death pathway in Down syndrome neurons. J Neurosci. 2005; 25:2295–2303. [PubMed: 15745955]

Kayed R, Head E, Sarsoza F, Saing T, Cotman CW, Necula M, Margol L, Wu J, Breydo L, Thompson JL, Rasool S, Gurlo T, Butler P, Glabe CG. Fibril specific, conformation dependent antibodies recognize a generic epitope common to amyloid fibrils and fibrillar oligomers that is absent in prefibrillar oligomers. Molecular neurodegeneration. 2007; 2:18. [PubMed: 17897471]

Knott AB, Perkins G, Schwarzenbacher R, Bossy-Wetzel E. Mitochondrial fragmentation in neurodegeneration. Nat Rev Neurosci. 2008; 9:505–518. [PubMed: 18568013]

Lott IT, Head E. Alzheimer disease and Down syndrome: factors in pathogenesis. Neurobiol Aging. 2005; 26:383–389. [PubMed: 15639317]

Pallardo FV, Lloret A, Lebel M, d'Ischia M, Cogger VC, Le Couteur DG, Gadaleta MN, Castello G, Pagano G. Mitochondrial dysfunction in some oxidative stress-related genetic diseases: Ataxia-Telangiectasia, Down Syndrome, Fanconi Anaemia and Werner Syndrome. Biogerontology. 2010; 11:401–419. [PubMed: 20237955]

Park KS, Wiederkehr A, Kirkpatrick C, Mattenberger Y, Martinou JC, Marchetti P, Demaurex N, Wollheim CB. Selective actions of mitochondrial fission/fusion genes on metabolism-secretion coupling in insulin-releasing cells. J Biol Chem. 2008; 283:33347–33356. [PubMed: 18832378]

Passos JF, Saretzki G, Ahmed S, Nelson G, Richter T, Peters H, Wappler I, Birket MJ, Harold G, Schaeuble K, Birch-Machin MA, Kirkwood TB, von Zglinicki T. Mitochondrial dysfunction accounts for the stochastic heterogeneity in telomere-dependent senescence. PLoS Biol. 2007; 5:e110. [PubMed: 17472436]

Roizen NJ, Patterson D. Down's syndrome. Lancet. 2003; 361:1281–1289. [PubMed: 12699967]

Slonim DK, Koide K, Johnson KL, Tantravahi U, Cowan JM, Jarrah Z, Bianchi DW. Functional genomic analysis of amniotic fluid cell-free mRNA suggests that oxidative stress is significant in Down syndrome fetuses. Proceedings of the National Academy of Sciences of the United States of America. 2009; 106:9425–9429. [PubMed: 19474297]

Valenti D, Manente GA, Moro L, Marra E, Vacca RA. Deficit of complex I activity in human skin fibroblasts with chromosome 21 trisomy and overproduction of reactive oxygen species by mitochondria: involvement of the cAMP/PKA signalling pathway. Biochem J. 2011; 435:679–688. [PubMed: 21338338]

Williams BR, Prabhu VR, Hunter KE, Glazier CM, Whittaker CA, Housman DE, Amon A. Aneuploidy affects proliferation and spontaneous immortalization in mammalian cells. Science. 2008; 322:703–709. [PubMed: 18974345]

Yu T, Robotham JL, Yoon Y. Increased production of reactive oxygen species in hyperglycemic conditions requires dynamic change of mitochondrial morphology. Proc Natl Acad Sci U S A. 2006; 103:2653–2658. [PubMed: 16477035]

Research Highlights

- Altered mitochondrial morphology in DS cells correlates with energy deficits
- Enforced mitochondrial activity increases oxidative stress and reduces DS cell viability
- The profile of gene expression in DS cells reflects chronic oxidative stress
- Adaptive mitochondrial downregulation compromises DS cell function

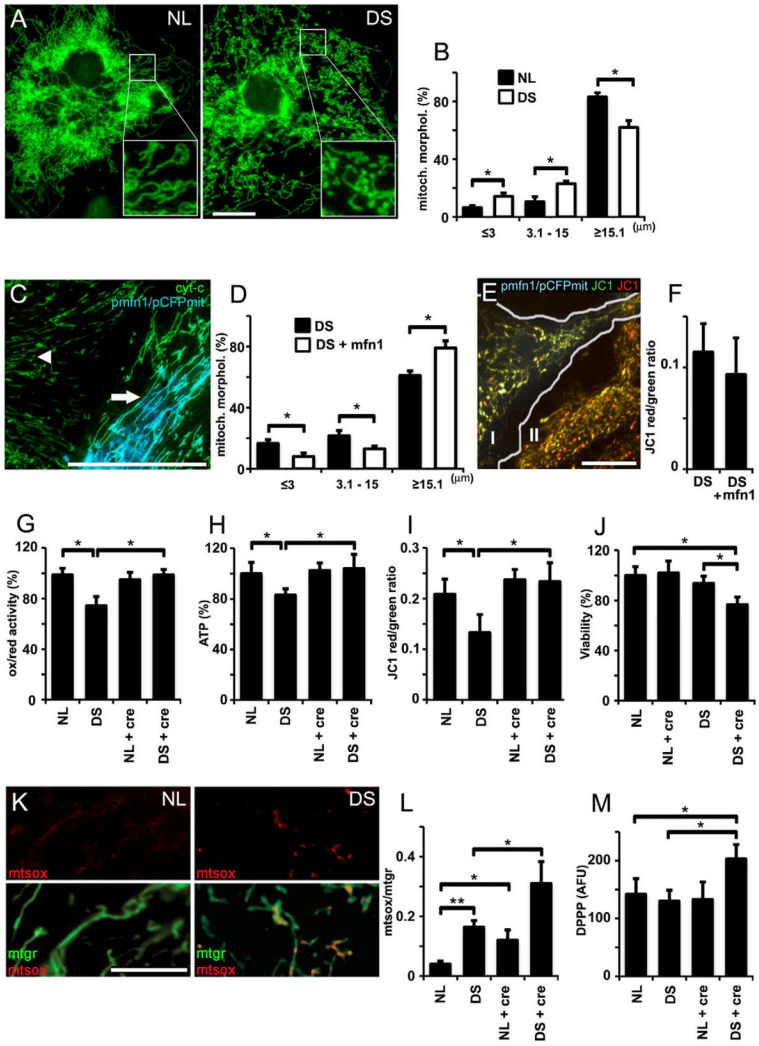

Figure 1. Mitochondrial alterations in DS astrocytes

(A) NL and DS astrocytes were stained with Mitotracker green. Elongated mitochondria predominate in NL astrocytes (NL; inset), while the number of puncta-like and globular mitochondria was higher in DS astrocytes (DS; inset). Scale bar: 10 μm.

(B) Quantification of mitochondrial shapes binned according to length/size in NL and DS astrocytes. *p<0.05

(C) A DS astrocyte (arrow) co-expressing mitofusin 1 (pmfn1) and cyan fluorescent protein targeted to mitochondria (pCFPmit) shows tubular mitochondria. In an adjacent, non-transfected DS cell (arrowhead), cytochrome C IF (green) illustrates shorter mitochondrial shapes. Scale bar: 20 μm.

(D) Morphometric analysis shows a higher frequency of longer mitochondria and lower frequency of shorter ones in mfn1-expressing DS astrocytes. *p<0.05

(E) A DS astrocyte cotransfected with pCFPmit and pmfn1 (I) shows longer mitochondria (JC-1 green) compared to a non trasnfected astrocyte (II). The number of energized mitochondria did not change (JC-1 red). Scale bar: 10 μm.

(F) JC-1 red/green ratio shows no differences in the frequency of energized mitochondria in pmfn1-expressing astrocytes compared to non transfected cells.

(G, H and I) Quantification of ATP, ox/red activity and MMP (red/green JC-1 fluorescence ratio). Treatment with 5 mM creatine (cre) markedly increased all three parameters of mitochondrial activity in DS astrocytes. $*p<0.01$.

(J) Quantification of astrocyte viability (LDH). Note the reduction in viability in DS astrocytes treated with creatine (5 mM). $*p<0.05$

(K) NL and DS astrocytes labeled with Mitotracker green and MitoSox. Simultaneous staining allows the visualization of superoxide production (mtsox, red) in live cell mitochondria (mtgr, green). Scale bars: 20 μm.

(L) Superoxide levels expressed as a MitoSOX/Mitotracker ratio (superoxide signal/total mitochondrial signal). Superoxide in DS mitochondria was further elevated by treatment with 5 mM creatine (NL+cre, DS+cre). *p<0.05 and **p<0.01

(M) Quantification of lipid peroxidation. DPPP was used to monitor lipid peroxidation, which is expressed as arbitrary fluorescent units (AFU). DS astrocytes treated with creatine (cre, 5 mM) exhibited a significant increase in lipid peroxidation (139% ± 11.2%) $*p<0.01$

Statistics: (B) and (D), by Student's t test; (G), (H), (I), (J), (L) and (N), by two way ANOVA followed by Tukey HSD test.

(G), (H), (I), (J), (L) and (M): values are the mean ± SD, $n=8$ independent experiments with cultures derived from different NL and DS brain specimens.

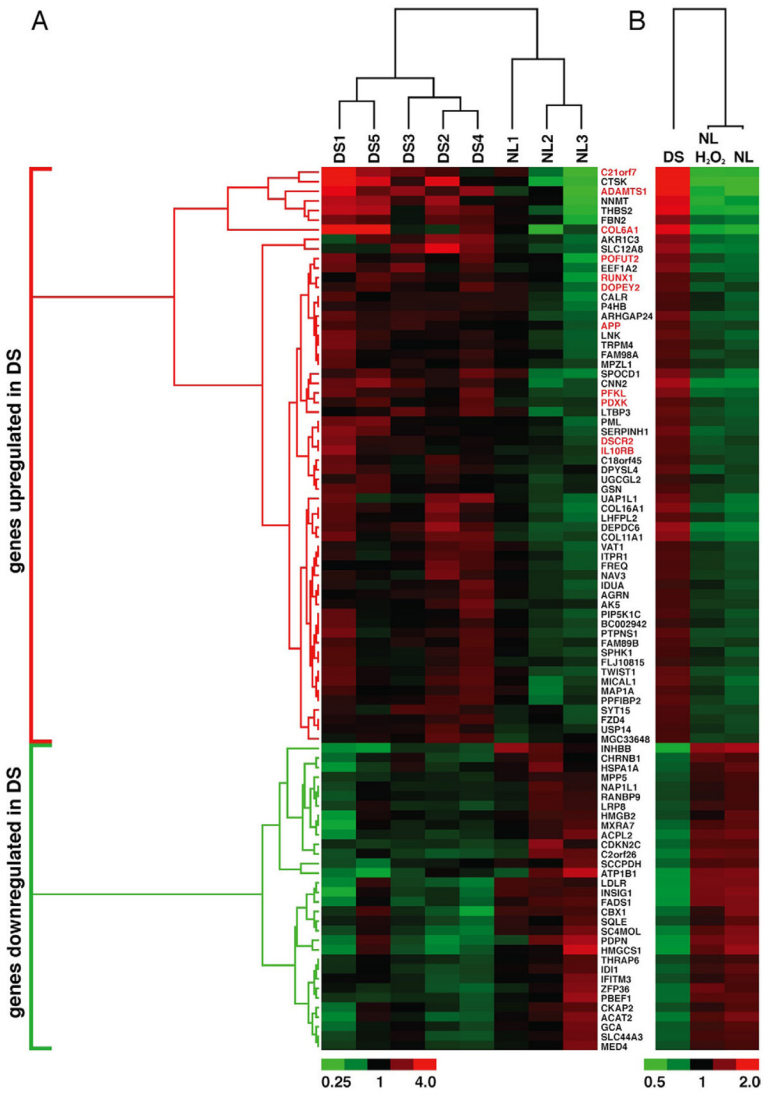

Figure 2. Gene expression in DS cells is associated with a pattern of chronic oxidative stress

Hierarchical cluster analysis. Relative RNA expression in 3 NL and 5 DS astrocyte cultures. Expression changes per gene with respect to the average expression across all arrays is shown as a heat map. Fold-change color code is indicated at the bottom. Distance trees represent relative difference (branching distance) between genes (left) or between conditions (top).

(A) 92 genes were differentially expressed in DS cells. The DS fingerprint segregated NL from DS samples, each of them derived from different cultures. Sixty genes were upregulated (red bracket), 12 of which are present in chr 21 (highlighted in red). 32 genes were downregulated (green bracket), none of which were located in chr 21.

(B) Relative RNA levels of the 92 genes in panel A. Average expression of the 3 NL and 5 DS cultures shown in (A)(NL and DS). NL+H_2O_2: average expression of the 3 NL cultures treated with H_2O_2 (see SMethods). Note that the expression of DS “signature” genes in H_2O_2-treated astrocytes shifts in the same direction as in DS cells.

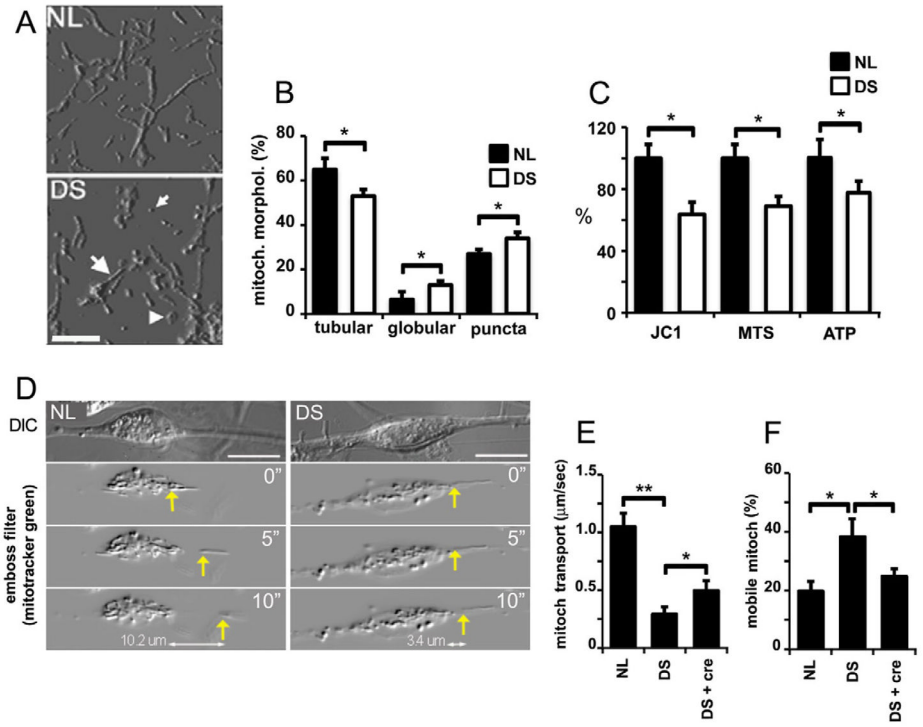

Figure 3. Altered mitochondrial morphology and function in DS neurons

(A) Mitochondria in NL and DS neurons (21 DIV) visualized with anti-cyt C antibody. Images were processed with an emboss filter. Mitochondria were classified as tubular (large arrow), puncta (small arrow), and globular (arrowhead). Scale bar: 5 μm.

(B) Quantification of mitochondrial morphotypes expressed as a percent of total mitochondrial mass. Tubular mitochondria are reduced while puncta- and globular-shaped mitochondria are increased in DS cells. $*p < 0.05$

(C) Reduced mitochondrial function in DS neurons. MMP is expressed as a JC-1 red/green ratio (JC-1). Ox/red activity (MTS) and ATP levels (ATP) were assessed using commercial assays. Results are expressed as a percent of the values found in NL cultures. DS cultures exhibit significant reductions in all three parameters. Values for each treatment were normalized to LDH cellular levels. $*p<0.05$

(D) Mitochondrial transport in NL and DS neurons (upper panel, DIC images) was recorded after live staining with Mitotracker green and processed with an emboss filter. Images correspond to 0, 5, and 10 sec respectively in both NL and DS neurons (yellow arrows). Travelled distance is specified in the bottom panel. Scale bar: 10 μm.

(E) Quantification of mitochondrial transport. DS mitochondria move slower than NL mitochondria. Creatine (5 mM; DS+cre) increased DS mitochondrial velocity (cre: 5 mM creatine). $*p<0.05$ and $**p<0.01$

(F) Quantification of mobile mitochondria. NL and DS neurons were labeled with Mitotracker green. Images acquired at 0 and 20 sec time-points were subtracted to generate a ratio of stationary over moving mitochondria (see SMethods). The number of moving mitochondria was higher in DS neurons and it was reduced to NL levels by treatment with 5 mM creatine (DS+cre) $*p<0.01$

Statistics: (B) and (C), by Student's t test; (E) and (F), by one way ANOVA followed by Tukey HSD test.

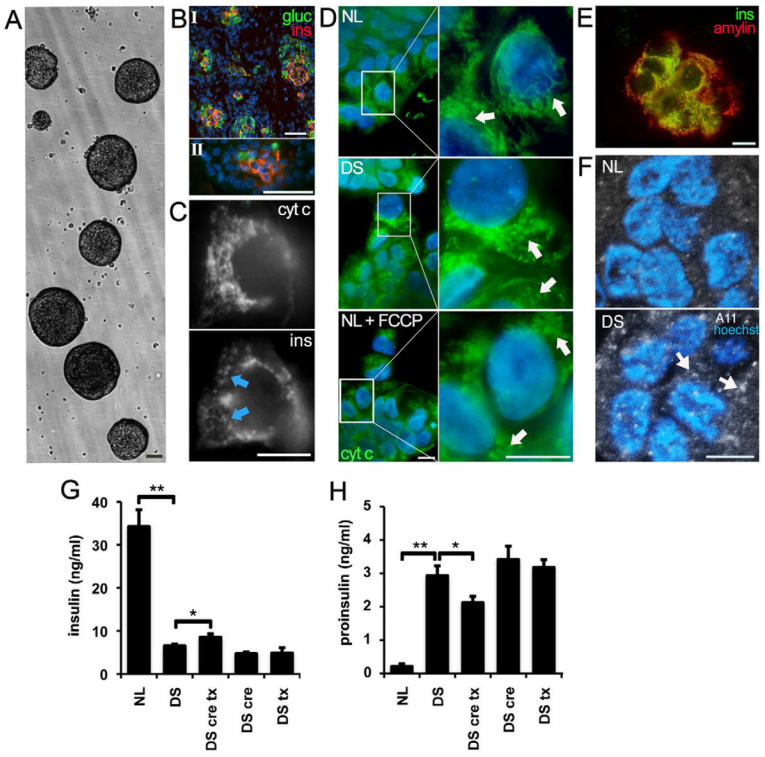

Figure 4. Altered mitochondrial morphology and function in DS pancreatic β cells

(A) Fetal human pancreatic cells were grown as floating islet cell clusters (ICC). NL and DS ICC exhibited similar expansion rates. Scale bar: 100 μm

(B) β cells from fetal pancreas (I) and ICC (II) express insulin (red) and glucagon (green). Scale bar: 100 μm

(C) Mitochondria visualized in an insulin-positive cell (ins, arrows) with anti-cytochorome C IF (cyt C). Scale bar: 10 μm

(D) Mitochondria were stained in β cells as described in panel C. Note the increase in fragmented mitochondria in DS ICCs and in NL ICC exposed to the electron transport chain uncoupler FCCP (NL+ FCCP). Scale bar: 10 μm

(E) Colocalization of insulin and IAPP (amylin) in ICC β cells. Scale bar: 10 μm

(F) A11 imunoreactivity in DS ICCs. Sections of NL and DS ICC were labeled with antibody A11, which recognizes IAPP oligomers. Note the increase in A11 staining in DS β cells (arrows). Nuclei were stained with DAPI. Scale bar: 10 μm

(G) Reduced basal insulin secretion in DS ICCs. Insulin secretion was measured in ICC conditioned medium. Note the small but significant increase in insulin secretion in DS ICC treated with 50 μM trolox and 5 mM creatine)(DS cre tx). $*p<0.05$ and $**p<0.01$

(H) Higher proinsulin secretion in DS ICC. Note the marked increase in proinsulin levels in CM of DS ICC. Combined trolox/creatine treatment reduced proinsulin secretion in DS ICC. $*p<0.05$ and $**p<0.01$

Statistics: (G) and (H), by one way ANOVA followed by Tukey HSD test. (G) and (H) values are the mean ± SD, $n=5$ independent experiments.